GL-TR-89-0171

A Multichannel Processing Approach to Real Time Network Detection, Phase Association and Threshold Monitoring

AD-A213 940

Frode Ringdal
Tormod Kvaerna

NTNF/NORSAR
Post Box 51
N-2007 Kjeller, NORWAY

31 May 1989

Scientific Report No. 1

APPROVED FOR PUBLIC RELEASE; DISTRIBUTION UNLIMITED

GEOPHYSICS LABORATORY
AIR FORCE SYSTEMS COMMAND
UNITED STATES AIR FORCE
HANSCOM AIR FORCE BASE, MASSACHUSETTS 01731-5000

SPONSORED BY
Defense Advanced Research Projects Agency
Nuclear Monitoring Research Office
ARPA ORDER NO. 5307

MONITORED BY
Geophysics Laboratory
Contract No. F49620-89-C-0038

This technical report has been reviewed and is approved for publication.

JAMES F. LEWKOWICZ
Contract Manager
Solid Earth Geophysics Branch
Earth Sciences Division

JAMES F. LEWKOWICZ
Branch Chief
Solid Earth Geophysics Branch
Earth Sciences Division

FOR THE COMMANDER

DONALD H. ECKHARDT, Director
Earth Sciences Division

Unclassified

SECURITY CLASSIFICATION OF THIS PAGE

REPORT DOCUMENTATION PAGE

Form Approved OMB No. 0704-0188

1a. REPORT SECURITY CLASSIFICATION Unclassified	1b. RESTRICTIVE MARKINGS
2a. SECURITY CLASSIFICATION AUTHORITY	3. DISTRIBUTION/AVAILABILITY OF REPORT Approved for public release; Distribution unlimited.
2b. DECLASSIFICATION/DOWNGRADING SCHEDULE	
4. PERFORMING ORGANIZATION REPORT NUMBER(S)	5. MONITORING ORGANIZATION REPORT NUMBER(S) GL-TR-89-0171
6a. NAME OF PERFORMING ORGANIZATION NTNF/NORSAR 6b. OFFICE SYMBOL (If applicable)	7a. NAME OF MONITORING ORGANIZATION Geophysics Laboratory
6c. ADDRESS (City, State, and ZIP Code) Post Box 51 N-2007 Kjeller, Norway	7b. ADDRESS (City, State, and ZIP Code) Hanscom Air Force Base Massachusetts 01731-5000
8a. NAME OF FUNDING/SPONSORING ORGANIZATION Defence Advanced Research Projects Agency 8b. OFFICE SYMBOL (If applicable) NMRO	9. PROCUREMENT INSTRUMENT IDENTIFICATION NUMBER Contract No. F49620-89-C-0038
8c. ADDRESS (City, State, and ZIP Code) 1400 Wilson Blvd. Arlington, VA 22209-2308	10. SOURCE OF FUNDING NUMBERS PROGRAM ELEMENT NO. 62714E PROJECT NO. 9A10 TASK NO DA WORK UNIT ACCESSION NO. BH

11. TITLE (Include Security Classification)
A Multichannel Processing Approach to Real Time Network Detection, Phase Association and Threshold Monitoring

12. PERSONAL AUTHOR(S)
Frode Ringdal and Tormod Kværna

13a. TYPE OF REPORT	13b. TIME COVERED	14. DATE OF REPORT (Year, Month, Day)	15. PAGE COUNT
SCIENTIFIC REP. 1	FROM 89/02/01 TO 89/04/30	1989 May 31	40

16. SUPPLEMENTARY NOTATION

17. COSATI CODES			18. SUBJECT TERMS (Continue on reverse if necessary and identify by block number)
FIELD	GROUP	SUB-GROUP	Network detection, phase association, threshold monitoring, regional arrays

19. ABSTRACT (Continue on reverse if necessary and identify by block number)

This paper presents an approach to multichannel processing of data recorded by a network of stations which represents an extension of the delay-and-sum beamforming traditionally applied in array processing. A number of geographical beam-steering points are defined, and for each beam a set of time-aligned traces derived from the network stations are processed together so as to extract, for each step in time, a set of features corresponding to that particular beam. Applying this approach to the network of the three regional arrays NORESS, ARCESS and FINESA in Fennoscandia, we demonstrate its usefulness for associating regional phases detected at individual arrays and originating from the same event. We also give an example of application addressing the problem of continuously monitoring the seismic noise field. In this regard, we show that one can obtain, at a given confidence level, a continuous assessment of the upper limit of magnitudes of seismic events that would go undetected by such a network.

20. DISTRIBUTION/AVAILABILITY OF ABSTRACT ☐ UNCLASSIFIED/UNLIMITED ☐ SAME AS RPT ☐ DTIC USERS	21. ABSTRACT SECURITY CLASSIFICATION UNCLASSIFIED	
22a. NAME OF RESPONSIBLE INDIVIDUAL James Lewkowicz	22b. TELEPHONE (Include Area Code) (617) 377-3028	22c. OFFICE SYMBOL GL/LWH

DD Form 1473, JUN 86 Previous editions are obsolete SECURITY CLASSIFICATION OF THIS PAGE

Preface

Under Contract No. F49620-C-89-0038, NTNF/NORSAR is conducting research within a wide range of subjects relevant to seismic monitoring. The emphasis of the research program is on developing and assessing methods for processing of data recorded by networks of small-aperture arrays and 3-component stations, for events both at regional and teleseismic distances. In addition, more general seismological research topics are addressed.

Each quarterly technical report under this contract will present one or several separate investigations addressing specific problems within the scope of the statement of work. Summaries of the research efforts within the program as a whole will be given in annual reports.

This Scientific Report No. 1 presents a manuscript entitled "A multichannel processing approach to real time network detection, phase association and threshold monitoring", by Frode Ringdal and Tormod Kværna.

A multichannel processing approach to real time network detection, phase association and threshold monitoring

FRODE RINGDAL AND TORMOD KVÆRNA
NTNF/NORSAR, Post Box 51, N-2007 Kjeller, Norway

Short Title: Multichannel processing of network data

Abstract

This paper presents an approach to multichannel processing of data recorded by a network of stations which represents an extension of the delay-and-sum beamforming traditionally applied in array processing. A number of geographical beam-steering points are defined, and for each beam a set of time-aligned traces derived from the network stations are processed together so as to extract, for each step in time, a set of features corresponding to that particular beam. Applying this approach to the network of the three regional arrays NORESS, ARCESS and FINESA in Fennoscandia, we demonstrate its usefulness for associating regional phases detected at individual arrays and originating from the same event. We also give an example of application addressing the problem of continuously monitoring the seismic noise field. In this regard, we show that one can obtain, at a given confidence level, a continuous assessment of the upper limit of magnitudes of seismic events that would go undetected by such a network.

Introduction

In the processing of seismic network data, individual phase detections corresponding to the same seismic event must be properly associated and grouped together. This is today usually done starting with an initial trial epicenter and then applying various search strategies supplemented by combinational techniques. For teleseismic monitoring using global network data, such techniques are well established, and a large degree of automation has been achieved (Goncz, 1980; Slunga, 1980).

In recent years, the subject of regional monitoring using networks comprising small-aperture arrays as well as single stations has attracted increased attention.

NORSAR Contribution No. 406

The motivation has been the need for improving the capability to monitor underground nuclear explosion testing down to very low magnitudes. The inclusion of regional phases in the phase association procedure leads to a considerable increase in the complexity of this task, and much effort has been devoted to developing automated procedures for handling this problem.

Techniques for automatic association of regional seismic phases recorded by a single array were first established in connection with the early NORESS array developments (Mykkeltveit and Ringdal, 1981; Mykkeltveit and Bungum, 1984). In later developments, knowledge-based system concepts were introduced, and the algorithms were expanded to include processing of data from a network of regional arrays and single stations (Bache, 1987; Baumgardt, 1987). Bratt and Bache (1988) developed an automated procedure for locating regional seismic events recorded by such a network, incorporating arrival times and azimuth information.

The emphasis of the phase association methods developed so far has been to build on the techniques previously applied successfully for global teleseismic networks, i.e., to associate individual phase detections at network stations using combinational techniques. Multichannel processing methods have received little attention, mainly because the signal coherency across extended networks is too low to make conventional beamforming useful. Incoherent beamforming (Ringdal *et al*, 1972; Husebye *et al*, 1972) has been suggested as a possible alternative approach. However, whereas this method is effective for networks of limited aperture, its practical usefulness for larger networks remains uncertain.

This paper presents a multichannel processing approach for network data that we have termed "generalized beamforming". In a sense, it represents not one single technique, but rather a framework for processing such data. Applying a procedure similar to the conventional delay-and-sum beamforming used in array processing, we define a number of geographical beam-steering points covering the region of interest. For each beam point, we obtain a set of time-aligned input traces, from which a set of beam features are continuously extracted. We show how this approach, in case of a regional network, can be used to associate individual phase detections corresponding to the same event. We also give an example of application addressing the problem of continuously monitoring the seismic noise level, for the purpose of obtaining a quantitative assessment of the upper limit of magnitudes of seismic events that would go undetected by such a network.

Method

In this section, we outline the overall approach to the problems addressed in this paper. We do not go into detail at this stage, but refer instead to subsequent sections discussing how the general framework can be used in practical application to various seismic monitoring problems.

Let us assume that a network of N seismic stations is available for monitoring a specified geographical region. For simplicity of presentation, we will assume that these are all array stations, able to provide phase velocity and azimuth information for detected signals. Extension to the single-station case is straightforward, although the quality of the results will naturally be reduced compared to when array stations are available.

We first subdivide the region to be monitored by introducing a grid of J geographical aiming points. Each such point then corresponds to a beam location, so that the beam set covers the entire region with a predefined spacing of the grid points.

For each station in the network, we assume that the recorded data are processed separately, using conventional algorithms. Specifically, let us denote by $s_{ijk}(T)$ the beam at the i'th array ($i = 1, 2, \ldots N$), steered toward the j'th beam point ($j = 1, 2, \ldots J$) and corresponding to the k'th seismic phase ($k = 1, 2, \ldots, K_{ij}$). Here, K_{ij} denotes the number of phases that might be of interest for the particular station-beam combination. We assume that these traces $s_{ijk}(T)$ are subjected to standard automatic detection processing, thus producing lists of signal onset times, phase velocity/azimuth estimates and other detection parameters, as well as noise level estimates during periods of non-detection.

In analogy with conventional array beamforming, the procedure is now to "steer" the network toward each beam location and process each beam individually by continuously extracting relevant features for that beam as a function of time.

The network beamsteering is done by computing a set of time delays τ_{ijk}, with indices defined as before, for all combinations of beams, stations and phases. Standard travel-time tables are used in these computations. Thus, for the j'th beam, we obtain a set of time-aligned channels:

$$\bar{s}_j(T) = \{s_{ijk}(T + \tau_{ijk})\} \quad k = 1, \ldots K_{ij}; \quad i = 1, \ldots, N \tag{1}$$

Here, $\bar{s}_j(T)$ can be viewed as a signal vector representing the individual station/phase observations corresponding to a hypothetical event with origin time T and located at the aiming point of the j'th beam.

Given this time alignment of the input traces, we now can proceed in several different ways to extract, as a function of time, characteris- tic features of the seismic field as seen when focusing on a specific beam area. One such approach is to consider the detector outputs on each individual trace and combine this information. In this case, the network beamforming process, for a given beam, at time T, can be described as looking for a pattern of detections/non-detections that matches the predicted pattern for a hypothetical event with origin time T and location within the beam region. The actual beam value is derived from probabilistic considerations, and in essence describes how well the observed pattern matches the prediction. By moving along the time axis, we thus obtain a beam trace that can be subjected to standard threshold algorithms for detection. The process can be supplemented by various individual "quality of fit" measures calculated at each time point. An example of this type of approach for the purpose of regional phase association is given in the following.

The generalized beamforming approach also provides a convenient tool to continuously assess the seismic noise field associated with a given beam. An application of particular interest in a monitoring situation would be to calculate, at each step in time, upper confidence limits for the magnitude of possible non-detected events for each beam. This would be useful to obtain a realistic assessment of actual network detection capabilities, at any given point in time. The paper presents an example of practical application of this approach.

Regional phase association

The method has been applied to a data base comprising 24 hours of recordings from the regional arrays NORESS, ARCESS and FINESA (Mykkeltveit *et al*, 1987; Korhonen *et al*, 1987; Kværna, 1989), with a beam deployment covering Fennoscandia and adjacent areas.

A RONAPP-type detector (Mykkeltveit and Bungum, 1984) was first applied to each array individually, using the broad-band F-K method (Kværna and Doornbos, 1986) to obtain phase velocity and azimuth for each detected phase. The resulting detection lists then provided the input to the network processor.

The beam grid used for network processing is shown in Figure 1, and comprises altogether 121 aiming points, approximately equally spaced. Typical distance between aiming points is 150 km.

In the network beamforming process, a simple model of assigning 0/1 probabilities to individual phases at each station was used. We required that estimated phase velocities, azimuth, dominant frequency and arrival times fall within predefined ranges for a phase detection to be accepted for a given beam. These tolerance ranges are specified in Table 1. Note in particular that only very general criteria are applied, and we have made no attempt to optimize performance by regionalization.

With this simplified model, the network beamforming process in practice was reduced to, for each beam and each time T, counting the number of phase matches for a hypothetical event located in the beam region and having origin time T. The detection threshold was set equal to 2. Thus, all occurrences of two or more matching phase detections were flagged as potential events. A typical beam trace is shown in Figure 2.

In analogy with conventional array processing, the beamforming procedure occasionally produces side lobe detections, thus resulting in several different beam detections for a given event. A grouping/ reduction process is therefore required.

The grouping procedure applied in our case consisted of successively linking together entries in the overall beam detection list. This was done in such a way that a new entry would be linked if it had at least one individual phase detection in common with a previous entry in the group. The maximum allowable duration of a group was set to 10 minutes (in practice, the longest duration was 7 minutes for this data set). In order to resolve obvious multiple events, groups were split up if two P-detections from the same array occurred with more than 30 seconds arrival time difference.

The results are summarized in Table 2. It is important to note that the total of 91 groups comprise *all* possible events that could be associated, given the station detection lists. Also, a scrutiny of the data shows that only 3 of these groups contain multiple events, all of these being small presumed mining explosions seen by one array only.

Some of the entries in Table 2, e.g., those generated from two secondary phases, are probably questionable seismic events, and even if real, may be impossible to locate accurately without access to additional data. An upper magnitude limit could be estimated for such events, in order to determine whether further detailed analysis is desirable. However, the large majority of the entries appear to correspond to real seismic events, and the grouping procedure facilitates the subsequent detailed analysis of the associated phases.

The network beamforming procedure gives an initial estimate of event location by selecting the "best beam" in each group. This is defined as the beam with the greatest number of associated phase detections, and if equality, the smallest average time residual of the detected phases. Since the initial beam grid is very coarse, we applied a beampacking algorithm for each detection group, using a grid spacing of 20 km in order to improve the location estimate. The resulting location estimates for the data set are displayed in Figure 3.

Table 3 lists the results of the automatic procedure, after beam- packing, for those events for which independent location estimates based on local network data were available. We note that the respective estimates are very consistent (median difference 40 km), and thus the beam results can be used as a reasonable first estimate of event location. For more accurate results, available techniques for accurate hypocenter location, e.g., the TTAZLOC procedure (Bratt and Bache, 1988)) should be used.

Continuous monitoring of upper event magnitude limits

As a second application of the generalized beamforming procedure, we now address the problem of monitoring the noise levels on each beam, and use this information to assess the size of events that might go undetected.

In formulating the approach, we consider a given geographical location, and a given "origin time" of a hypothetical event. Assume that N seismic phases are considered (there might be several stations and several phases per station).

For each phase, we assume that we have an estimate S_i of the signal (or noise) level at the predicted arrival time. For P-phases, S_i might be the maximum short term average (STA) value (1 second integration window) within $\pm$ 5 seconds of the predicted time. For Lg, a longer STA integration window (e.g., 10 seconds) might be used, and its maximum might be selected allowing a somewhat greater deviation from the predicted arrival time.

We assume that the network has been calibrated (or alternatively that standard attenuation values are available), so that magnitude correction factors (b_i) are available for all phases. Thus, if a detectable signal is present:

$$m_i = log(S_i) + b_i \quad (i = 1,2,\ldots N) \tag{2}$$

Here, m_i are estimates of the event magnitude m. Statistically, we can consider each m_i as sampled from a normal distribution (m,σ). Based on NORSAR experience, we consider a standard value of $\sigma = 0.2$ to be reasonable for a small epicentral area, and this value will be used in the following.

Let us now assume a "noise situation", i.e., that there are no phase detections corresponding to events at the given location for the given origin time.

We then have a set of "noise" observations a_i, where

$$a_i = log(S_i) + b_i \quad (i = 1,2,\ldots N) \tag{3}$$

If a hypothetical event of magnitude m were present, it would have phase magnitudes m_i normally distributed around m. We know that for each phase,

$$m_i \leq a_i \quad (i = 1,2,\ldots N) \tag{4}$$

Following a procedure similar to that of Ringdal (1976), we now consider the function:

$$f(m) = \text{Prob(all } m_i \leq a_i \text{ / event magnitude } m) \tag{5}$$

For each phase, we obtain probability functions $f_i(m)$ and $g_i(m)$ as follows:

$$f_i(m) = \text{Prob}(m_i \leq a_i/m) = 1 - \Phi(\frac{m - a_i}{r}) \quad (i = 1,2,\ldots N) \tag{6}$$

$$g_i(m) = \text{Prob}(m_i > a_i/m) = \Phi(\frac{m - a_i}{r}) \quad (i = 1,2,\ldots N) \tag{7}$$

where Φ is the standard (0,1) normal distribution.

Thus, assuming independence,

$$f(m) = \prod_{i=1}^{N} f_i(m) \tag{8}$$

The probability $g(m)$ that at least one of the observed noise values would be exceeded by the signals of a hypothetical event of magnitude m, then becomes

$$g(m) = 1 - f(m) \tag{9}$$

As illustrated in Figure 4, the 90 per cent upper limit is then defined as the solution of the equation

$$g(m) = 0.90 \tag{10}$$

It is important to interpret the 90 per cent limit defined above in the proper way. Thus, it should not be considered as a 90 per cent network detection threshold since we have made no allowance for a signal-to-noise ratio which would be required in order to detect an event, given the noise levels. Rather, the computed level is tied to the actually observed noise values, and to the fact that any hypothetical signal must lie below these values. Our 90 per cent limit represents the largest magnitude of a possible hidden event, in the sense that above this limit, there is at least a 90 per cent probability that one or more of the observed noise values would be exceeded by the signals of such an event.

As an application of the method, we selected an area as shown in Figure 5 situated at similar distance from the three arrays. For each of the three arrays, one Pn beam and one Lg beam were steered to this location. The beam traces were filtered using the frequency bands 3-5 Hz (Pn) and 2-4 Hz (Lg). Magnitude calibration values (b_i) were obtained by processing previously recorded events of known magnitude (M_L) and at similar distance ranges, and then determining b_i values independently for Pn and Lg.

Based on these input traces from the three arrays, a network beam was then formed, using time delays for each phase that corresponded to the given location. Arrival time tolerances were set to ± 5 seconds for Pn and ± 10 seconds for Lg. This is roughly consistent with a beam radius of 50 km as shown on the figure. STA integration windows were set to 1 second for Pn and 10 seconds for Lg. The values of Si in eq. (2) were obtained as the maximum STA values within the respective arrival time tolerances, using the mid-point of the integration interval as time reference.

We chose to analyze a 3 1/2 hour interval during which four regional seismic events of $M_L > 2.0$ were reported in the Helsinki bulletin. These events were all located outside the beam region to be studied, and one of our aims was to investigate how interfering signals from these events would influence the monitoring capability for the chosen beam region.

Figure 6 shows, for the beam region considered, the computed 90 per cent upper magnitude limits, plotted as a function of time. In this figure, only the Pn phase has been used, and the three arrays are shown individually and in combination (bottom trace).

It is clear from Figure 6 that when considering individual arrays only, there are several possible time intervals when relatively large events ($M_L \sim 2.0$-3.0) located in the beam area might go undetected because of signals from interfering events. However, when the Pn phases are combined, these instances occur much more seldom.

Figure 7 shows a similar plot, but this time including both the Pn and the Lg phase for each array. Even on an individual array basis, this causes substantial reduction in the upper magnitude limits. For the combined plot (bottom trace of Figure 7), which takes into account all 6 Pn and Lg phases from the three arrays, we see that the upper limit is well below $M_L = 2.0$ for the entire time interval. Thus, we may conclude that, at the specified level of confidence, no event of $M_L = 2.0$ or higher occurred in the beam region during the time period considered.

Discussion

With regard to phase association, the generalized beamforming approach presented in this paper provides an effective method to group all combinations of individual phase detections that could possibly correspond to the same seismic event. At the same time, preliminary estimates of epicenter and origin time are obtained.

The primary importance of this would be to obtain a starting point for subsequent detailed interactive analysis aimed at precise determination of source parameters. In particular, expert system approaches (either script-based or rule-based) could be invoked at this stage. The advantage of applying the generalized beamforming as the first step is to reduce the amount of combinational processing that would be necessary otherwise. It is here noteworthy that the processing load when applying beamforming increases in a linear fashion when the number of individual phase detections increase, whereas combinational possibilities tend to increase exponentially. While we have in this paper used only a three-array network, the extension to larger networks is clearly straightforward.

The application of the method to provide continuous monitoring of upper magnitude limits at specified beam locations provides a useful supplement to standard statistical network capability studies (e.g., Wirth, 1977; Ringdal, 1986). In particular, this application would give a way to assess the possible magnitude of non-detected events during the coda of large earthquakes. In such situations, it would be appropriate to use global network data and include as many relevant phases as possible for each network station. For example, while an expected P phase at a given station may be obscured by the earthquake coda, later phases such as PcP or PP may be less influenced, and the noise level at their respective expected arrival times would therefore provide important information as to the size of possible undetected events.

As a final comment, we note that the approach presented here to upper limit magnitude calculation could be applied to extend the utility of various discriminants, such as M_s:m_b. For small explosions, surface waves frequently are too weak to be observed at any station of the recording network. Obtaining reliable upper bound on M_s in such cases would expand the range of usefulness of this discriminant. In practice, an "upper bound" for single-station measurements has often been given as the "noise magnitude" at that station, i.e., the M_s value that corresponds to the actually observed noise level at the expected time of Rayleigh wave arrival. The proposed procedure will include this as a special case of a more general network formulation.

In future studies, we plan to investigate the application of more sophisticated probabilistic models in the generation of beam traces and the continuous extraction of features associated with the individual beams. Application to larger networks, including teleseismic monitoring using global network data, will also be considered.

Acknowledgement

This research has been sponsored by the Defense Advanced Research Project Agency (DARPA) and monitored by the Air Force Geophysical Laboratory (AFGL) under Contract No. F49620-89-C-0038.

References

[1] Bache, T.C. (1987): A knowledge-based system for analyzing data from a network of NORESS-type arrays. Papers presented at 9th DARPA/AFGL Research Symposium, 15-18 June, 167- 172.

[2] Baumgardt, D.R. (1987): Case-based reasoning applied to regional seismic event characterization. Papers presented at 9th DARPA/AFGL Research Symposium, 15-18 June, 173-178.

[3] Bratt, S.R. and T.C. Bache (1988): Locating events with a sparse network of regional arrays. Bull. Seism. Soc. Am., 78, 780- 798.

[4] Goncz, J.H. (1980): Present status and dynamic planning for automatic association programs. Teledyne Geotech Report SDAC- TR-80-2.

[5] Husebye, E.S., F. Ringdal and J. Fyen (1972): On real- time processing of data from a global seismological network. NORSAR Tech. Rep. No. 43, Kjeller, Norway.

[6] Korhonen, H., S. Pirhonen, F. Ringdal, S. Mykkeltveit, T. Kværna, P.W. Larsen and R. Paulsen (1987): The FINESA array and preliminary results of data analysis. Report S-16, Inst. of Seismology, University of Helsinki, Helsinki, Finland.

[7] Kværna, T. and D.J. Doornbos (1986): An integrated approach to slowness analysis with arrays and three-component seismometers. *In:* NORSAR Scientific Report 2 85/86, Kjeller, Norway.

[8] Kværna, T. (1989): On exploitation of small-aperture NORESS type arrays for enhanced P-wave detectability. Bull. Seism. Soc. Am., 79 (in press).

[9] Mykkeltveit, S. and F. Ringdal (1981): Phase identification and event location at regional distances using small- aperture array data. *In:* Identification of Seismic Sources – Earthquake or Underground Explosion, E.S. Husebye and S. Mykkeltveit, Editors, D. Reidel Publ. Co., Dordrecht, Holland, 467-481.

[10] Mykkeltveit, S. and H. Bungum (1984): Processing of seismic events using data from small-aperture arrays. Bull. Seism. Soc. Am., 74, 2313-2333.

[11] Mykkeltveit, S., F. Ringdal, J. Fyen and T. Kværna (1987): Initial results from analysis of data recorded at the new regional array in Finnmark, Norway. *In:* NORSAR Sci. Rep. No. 1-87/88, Kjeller, Norway.

[12] Ringdal, F., E.S. Husebye and A. Dahle (1972): Event detection problems for a partially coherent array. NORSAR Tech. Rep. No. 45, Kjeller, Norway.

[13] Ringdal, F. (1976): Maximum-likelihood estimation of seismic magnitude. Bull. Seism. Soc. Am., 66, 789-802.

[14] Ringdal, F. (1986): Study of magnitudes, seismicity and earthquake detectability using a global network. Bull. Seism. Soc. Am., 76, 1641-1659.

[15] Slunga, R. (1980): International Seismological Data Center. An algorithm for associating reported arrivals to a global seismic network into groups defining events. FOA Report C 20386- T1, Stockholm, Sweden.

[16] Wirth, M.H. (1977): Estimation of network detection and location capability. Teledyne Geotech, Alexandria, Virginia.

Table Captions

Table 1. Acceptance limits for parameters used in the network beamforming process, as applied in the example described in the text.

Table 2. Phase groups associated by the network beamforming procedure for a 24-hour interval, based on NORESS/ARCESS/FINESA detection lists.

Table 3. Location estimates obtained automatically from the beampacking procedure compared with independent network locations from the Helsinki and Bergen bulletins. Note the good consistency, especially for events with more than one detecting array.

Figure Captions

Fig. 1. Beam grid used in the generalized beamforming procedure for the purpose of associating regional phases from NORESS, ARCESS and FINESA. The location of the three arrays is shown on the map.

Fig. 2. Illustration of the beamforming procedure, using 0/1 weights for individual phase detections as described in the text. For each of the three arrays, detection time traces for Pn and Lg are displayed in the form of step functions. A value of 1 for these functions indicates that an acceptable detection (with regard to azimuth, phase velocity, etc.) has occurred within a specified time window. To illustrate the beam delays, an arbitrary origin time T has been marked on the beam trace, and the predicted arrival times corresponding to a hypothetical event at the beam location with origin time T are marked as arrows. The network beam (top trace) is a sum of the time-aligned individual traces, including the Pg and Sn phases, which are not shown on the plot.

Fig. 3. Event location results, after beampacking, for the phase groups associated by the network beamforming algorithm. The location of the three arrays NORESS, ARCESS, FINESA is also shown.

Fig. 4. Illustration of the procedure for calculating upper magnitude limits. Each network station gives rise to a probability distribution $g_i(M)$ as described in the text. The dotted curve, $g(M)$, represents the probability, given event magnitude M, that the signal from a hypothetical event would exceed the actually observed noise level at at least one station.

Fig. 5. Location of the beam area used in the example of continuous monitoring of upper magnitude limits on non-detected events. The area covers a circle of approximately 50 km radius, and is situated at similar distances from the three arrays.

Fig. 6. Results from the continuous threshold monitoring of the area shown in Figure 3 for a 3 1/2 hour period, using Pn phases only. The top three traces show, for each array, the largest magnitude of a possible non-detected event (confidence 90 per cent) as a function of time. The bottom trace shows the result of combining the observations from all three arrays (Pn phase only) as described in the text.

Fig. 7. Same as Figure 6, but using both the Pn and Lg phases for the upper magnitude limit calculations. Comparing with Figure 6, we note that this serves to lower the thresholds, both for each individual array (top three traces) and for the combined results (bottom trace).

Table 1

	Phase Type				
	Pn	Pg	Sn	Lg	Rg
Distance interval[1] (km) for which a phase is accepted	160-3000	0-600	160-3000	0-2000	0-400
Maximum allowable deviation from predicted arrival time (s)	15	20	30	35	40
Maximum allowable azimuth deviation (degrees)	20	20	20	20	20
Acceptance limits for apparent phase velocity (km/s)	5.8-14	5.8-10	3.2-5.8	3.0-5.0	2.5-3.7
Acceptance limits[2] for dominant frequency (Hz)	0.5-20	0.5-20	0.5-20	0.5-20	0.5-20

1) For NORESS, the Rg phase is not included in the phase table

2) For FINESA, a lower frequency limit of 0.9 Hz is used for all phases.

Table 2

Number of phase groups:		Number of phases for best beam in each group: 2	3	4	5	6	7	8
NORESS only	18	13	4	1	0	0	0	0
ARCESS only	34	19	10	4	1	0	0	0
FINESA only	14	13	1	0	0	0	0	0
Two arrays	17	9	4	3	0	1	0	0
Three arrays	8	0	0	2	0	1	3	2
Totals	91	54	19	10	1	2	3	2

Table 3

Event No.	Date	Time	Network Lat.	Network Lon.	Mag. M_L	No. of phases	No. of arrays	Beamforming Lat.	Beamforming Lon.	'Error' (km)
1	88/03/17	08.40.25.0	57.73	11.03	2.5	7	3	57.9	10.4	39
2	"	08.46.18.7	58.07	11.36	2.6	6	2	57.9	10.8	36
3	"	09.07.10.3	58.08	11.43	2.7	8	3	57.8	10.8	47
4	"	10.21.23.0	69.6	29.9	2.9	8	3	69.6	30.5	23
5	"	10.27.20.0	59.2	27.6	2.3	4	2	59.5	27.5	34
6	"	10.46.21.0	59.2	27.6	<2	2	1	59.8	28.7	90
7	"	11.18.48.0	59.3	27.2	2.3	5	3	58.9	26.7	52
8	"	11.54.41.0	65.8	24.7	<2	5	1	66.6	24.4	89
9	"	11.57.57.9	60.57	8.36	1.8	2	1	60.6	8.1	14
10	"	12.02.36.0	59.4	28.5	2.1	3	2	59.5	28.2	20
11	"	12.42.22.9	59.78	10.76	2.3	3	1	59.5	10.0	52
12	"	14.13.14.0	58.33	6.28	2.4	4	1	58.0	6.1	38
13	"	14.21.08.0	60.9	29.4	2.3	3	2	61.3	29.1	47
14	"	14.33.58.3	59.06	5.88	2.2	2	1	58.9	3.3	144
15	"	18.58.08.1	59.68	5.57	3.2	7	3	60.0	5.7	36

Figure 1

Initial beam grid

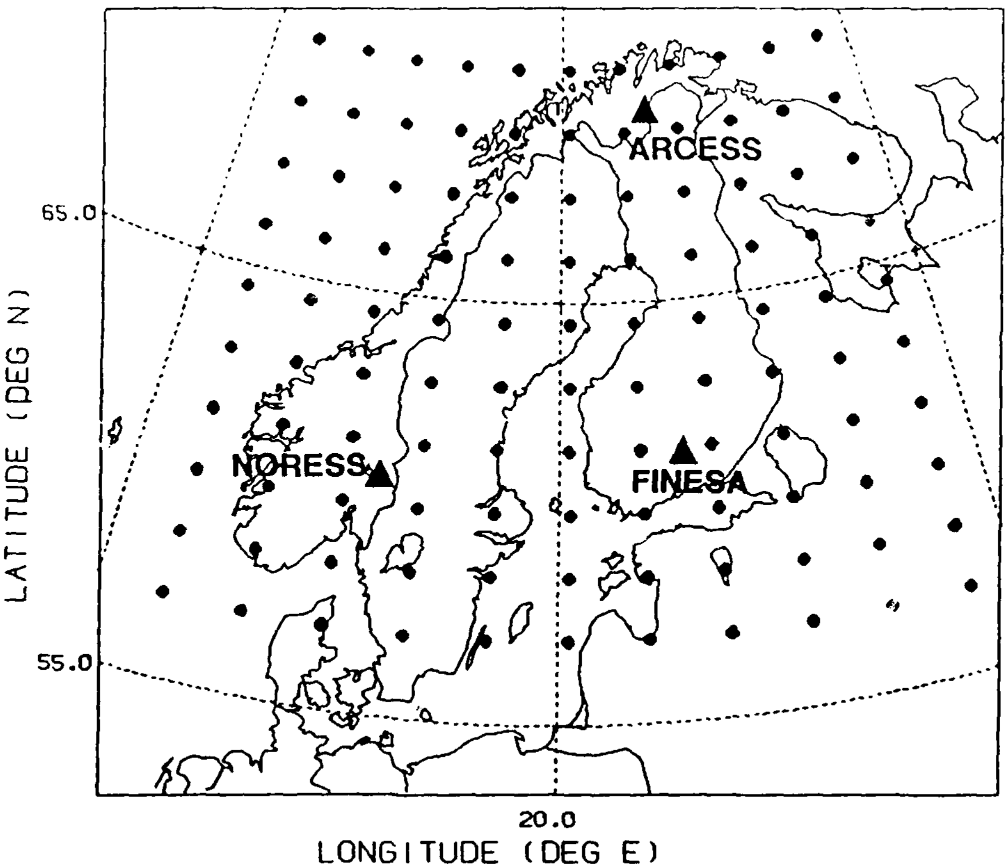

Figure 2

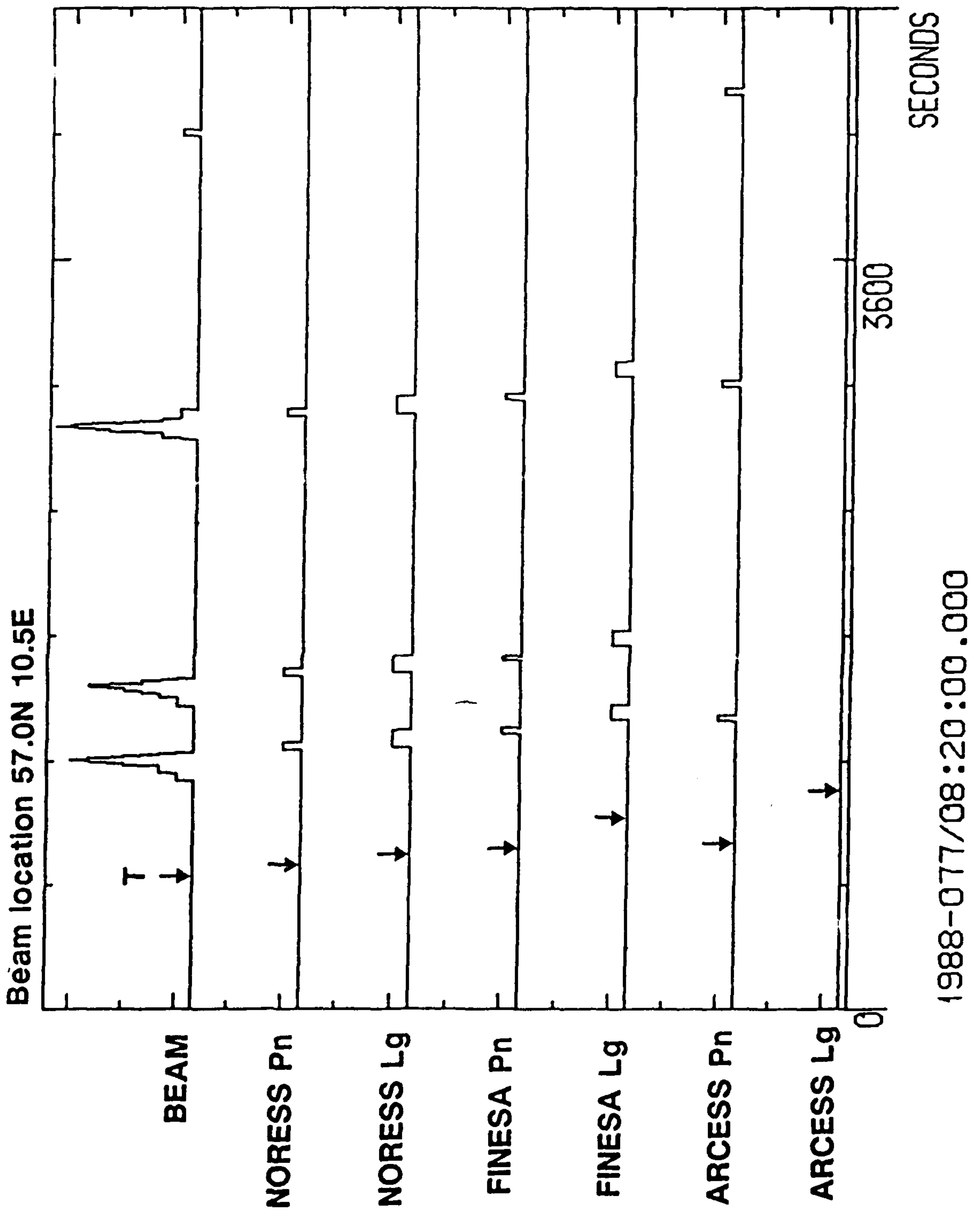
Beam location 57.0N 10.5E
T
BEAM
NORESS Pn
NORESS Lg
FINESA Pn
FINESA Lg
ARCESS Pn
ARCESS Lg
0
3600
SECONDS
1988-077/08:20:00.000

Figure 3

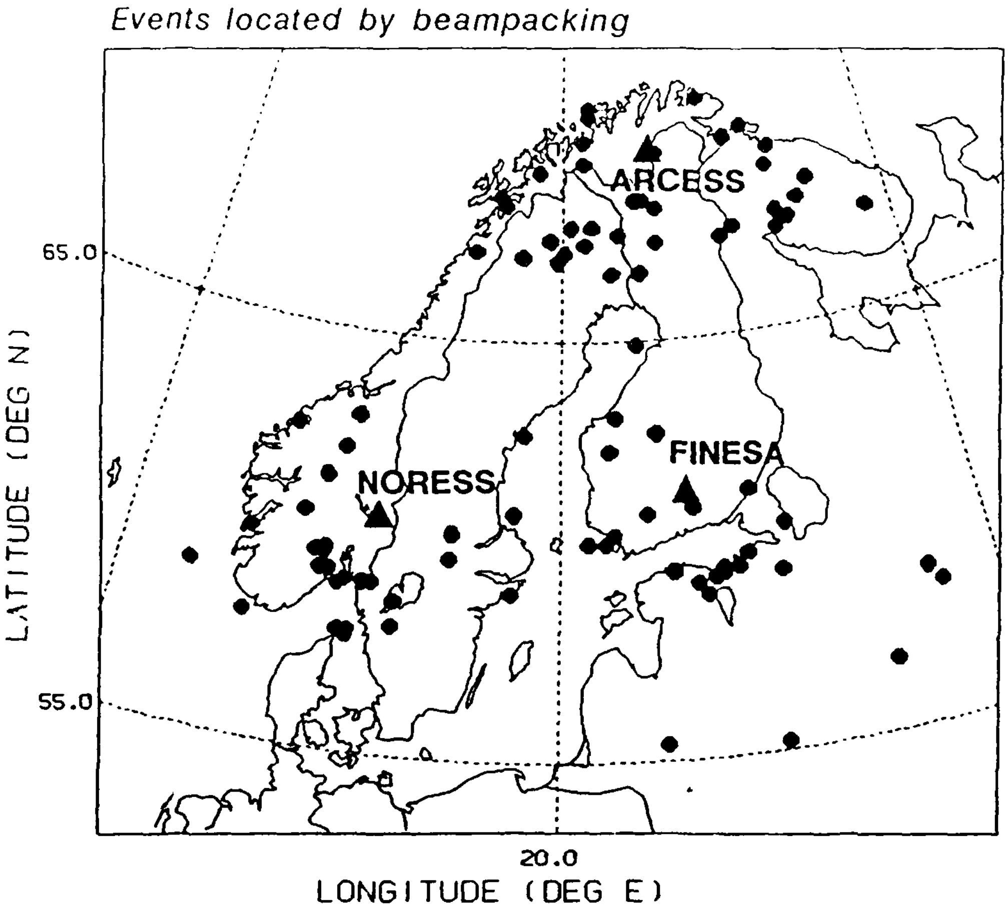
Events located by beampacking
ARCESS
NORESS
FINESA
65.0
55.0
20.0
LATITUDE (DEG N)
LONGITUDE (DEG E)

Figure 4

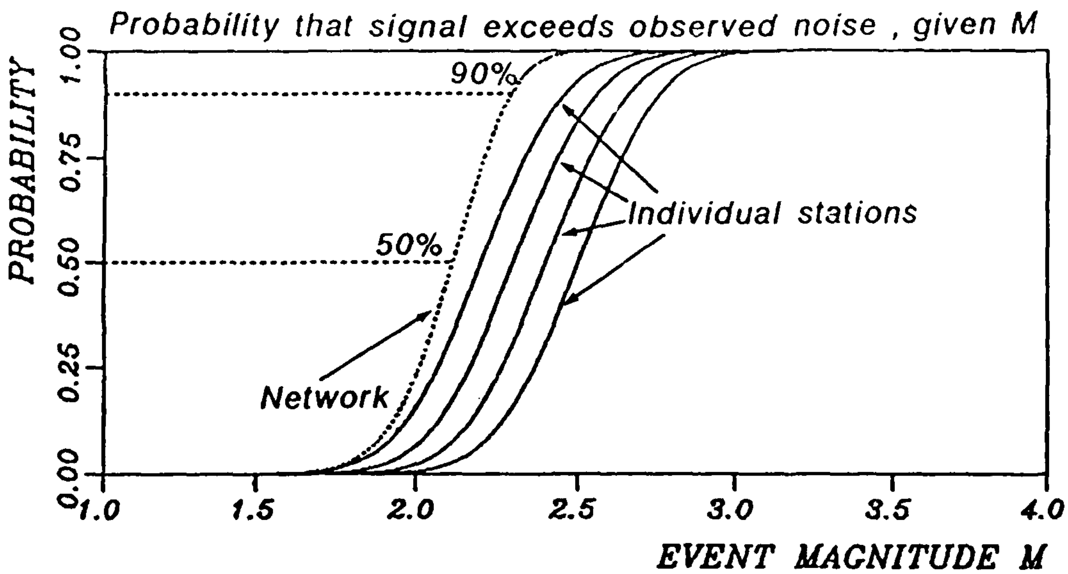

Probability that signal exceeds observed noise , given M
PROBABILITY
0.00
0.25
0.50
0.75
1.00
90%
50%
Individual stations
Network
1.0
1.5
2.0
2.5
3.0
3.5
4.0
EVENT MAGNITUDE M

Figure 5

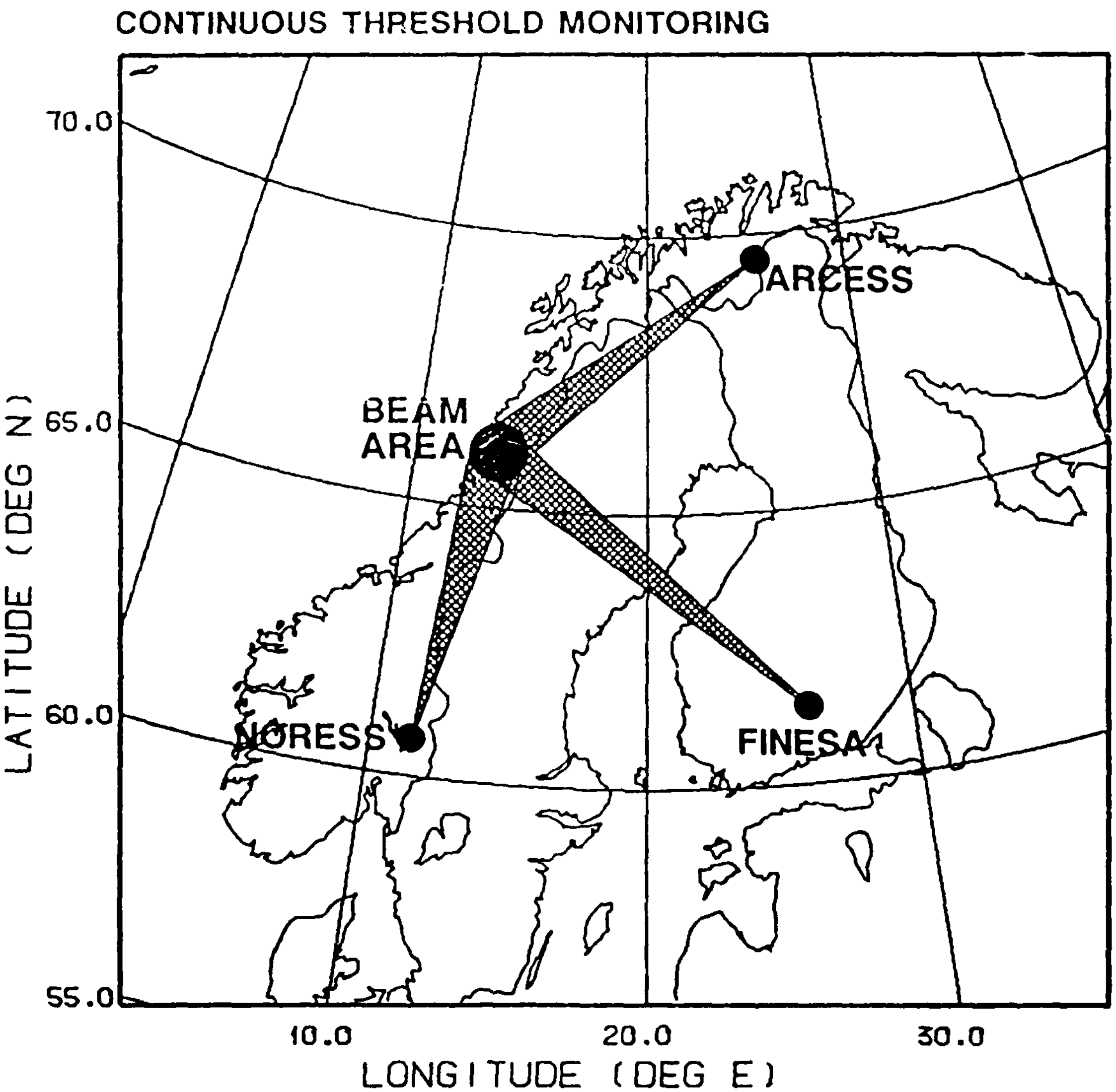
CONTINUOUS THRESHOLD MONITORING
70.0
65.0
60.0
55.0
LATITUDE (DEG N)
10.0
20.0
30.0
LONGITUDE (DEG E)
ARCESS
BEAM
AREA
NORESS
FINESA

Figure 6

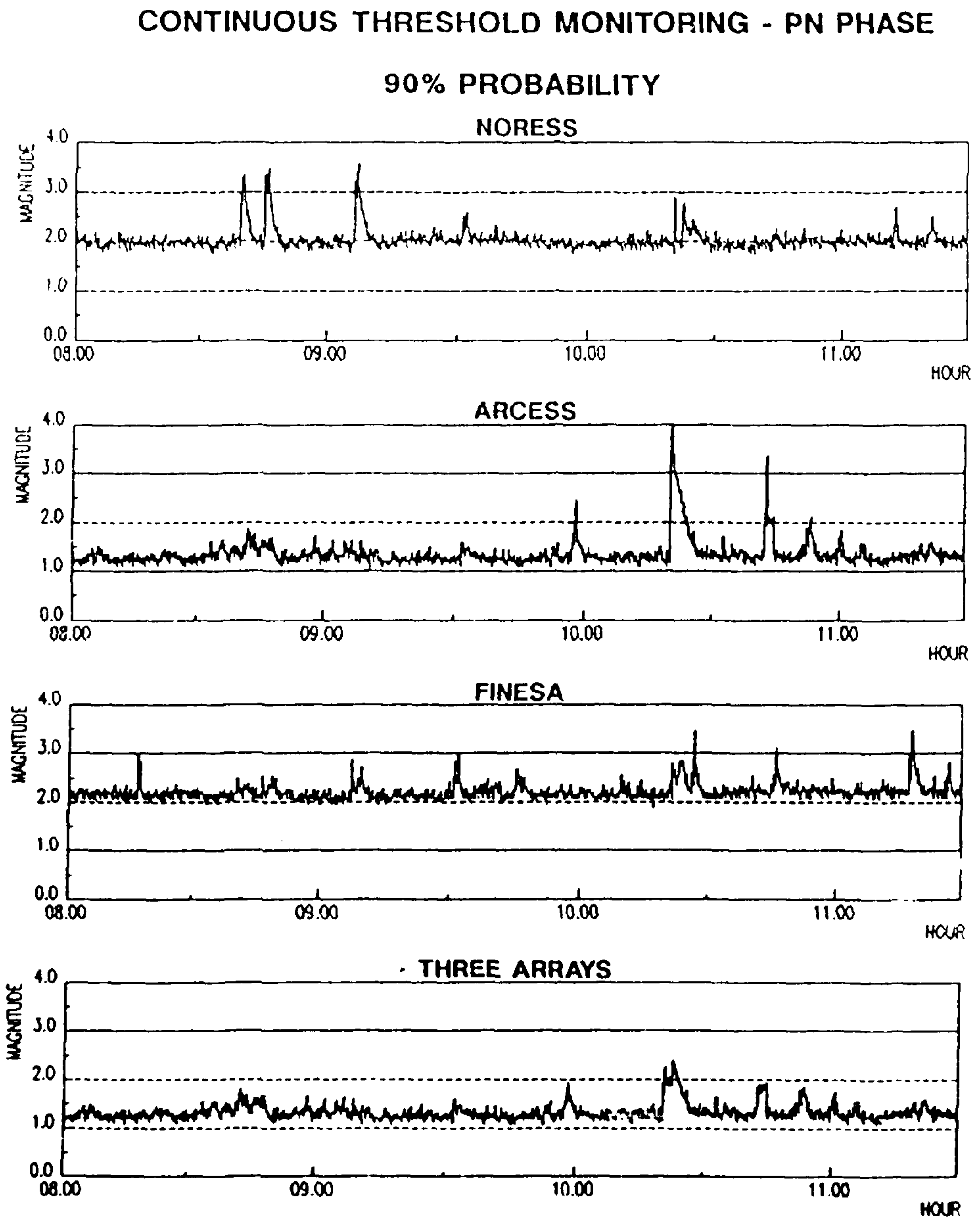
CONTINUOUS THRESHOLD MONITORING - PN PHASE
90% PROBABILITY
NORESS
ARCESS
FINESA
THREE ARRAYS
MAGNITUDE
4.0
3.0
2.0
1.0
0.0
08.00
09.00
10.00
11.00
HOUR

Figure 7

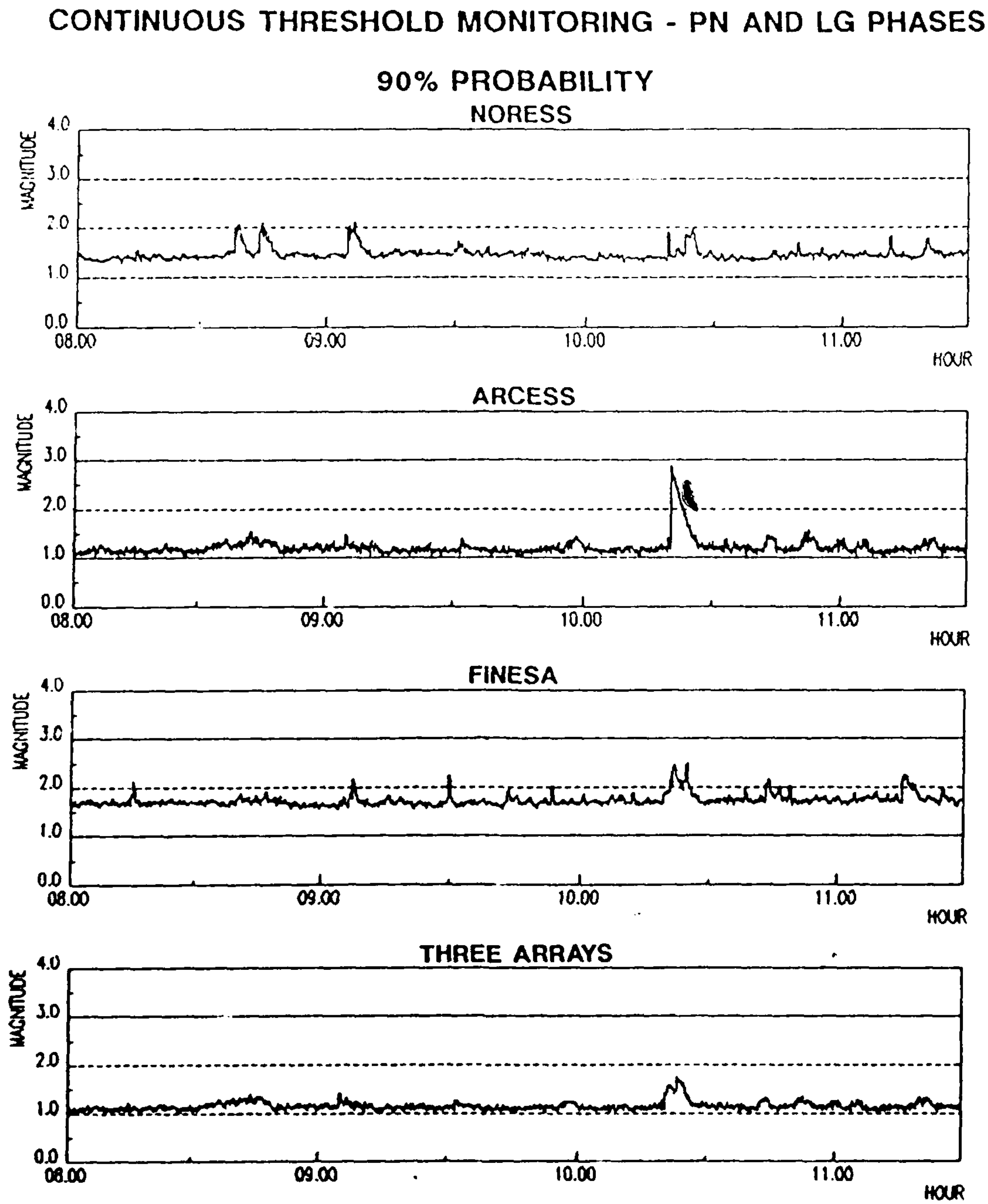

CONTINUOUS THRESHOLD MONITORING - PN AND LG PHASES
90% PROBABILITY
NORESS
MAGNITUDE
4.0
3.0
2.0
1.0
0.0
08.00
09.00
10.00
11.00
HOUR
ARCESS
MAGNITUDE
4.0
3.0
2.0
1.0
0.0
08.00
09.00
10.00
11.00
HOUR
FINESA
MAGNITUDE
4.0
3.0
2.0
1.0
0.0
08.00
09.00
10.00
11.00
HOUR
THREE ARRAYS
MAGNITUDE
4.0
3.0
2.0
1.0
0.0
08.00
09.00
10.00
11.00
HOUR

CONTRACTORS (United States)

Professor Keiiti Aki
Center for Earth Sciences
University of Southern California
University Park
Los Angeles, CA 90089-0741

Professor Thomas Ahrens
Seismological Lab, 252-21
Div. of Geological & Planetary Sci.
California Institute of Technology
Pasadena, CA 91125

Professor Charles B. Archambeau
Cooperative Institute for Resch
in Environmental Sciences
University of Colorado
Boulder, CO 80309

Dr. Thomas C. Bache Jr.
Science Applications Int'l Corp.
10210 Campus Point Drive
San Diego, CA 92121 (2 copies)

Dr. Muawia Barazangi
Institute for the Study of
of the Continent
Cornell University
Ithaca, NY 14853

Dr. Douglas R. Baumgardt
Signal Analysis & Systems Div.
ENSCO, Inc.
5400 Port Royal Road
Springfield, VA 22151-2388

Dr. Jonathan Berger
ICPP, A-205
Scripps Institution of Oceanography
University of California, San Diego
La Jolla, CA 92093

Dr. S. Bratt
Science Applications Int'l Corp.
10210 Campus Point Drive
San Diego, CA 92121

Dr. Lawrence J. Burdick
Woodward-Clyde Consultants
P.O. Box 93245
Pasadena, CA 91109-3245 (2 copies)

Professor Robert W. Clayton
Seismological Laboratory/Div. of
Geological & Planetary Sciences
California Institute of Technology
Pasadena, CA 91125

Dr Karl Coyner
New England Research, Inc.
76 Olcott Drive
White River Junction, VT 05001

Dr. Vernon F. Cormier
Department of Geology & Geophysics
U-45, Room 207
The University of Conneticut
Storrs, Connecticut 06268

Dr. Steven Day
Dept. of Geological Sciences
San Diego State U.
San Diego, CA 92182

Dr. Zoltan A. Der
ENSCO, Inc.
5400 Port Royal Road
Springfield, VA 22151-2388

Professor John Ferguson
Center for Lithospheric Studies
The University of Texas at Dallas
P.O. Box 830688
Richardson, TX 75083-0688

Professor Stanley Flatte'
Applied Sciences Building
University of California,
Santa Cruz, CA 95064

Dr. Alexander Florence
SRI International
333 Ravenswood Avenue
Menlo Park, CA 94025-3493

Professor Steven Grand
University of Texas at Austin
Dept of Geological Sciences
Austin, TX 78713-7909

Dr. Henry L. Gray
Associate Dean of Dedman College
Department of Statistical Sciences
Southern Methodist University
Dallas, TX 75275

Professor Roy Greenfield
Geosciences Department
403 Deike Building
The Pennsylvania State University
University Park, PA 16802

Dr. Indra N. Gupta
Teledyne Geotech
314 Montgomery St.
Alexandria, VA 22314

Professor David G. Harkrider
Seismological Laboratory
Div of Geological & Planetary Sciences
California Institute of Technology
Pasadena, CA 91125

Professor Donald V. Helmberger
Seismological Laboratory
Div of Geological & Planetary Sciences
California Institute of Technology
Pasadena, CA 91125

Professor Eugene Herrin
Institute for the Study of Earth
and Man/Geophysical Laboratory
Southern Methodist University
Dallas, TX 75275

Professor Robert B. Herrmann
Department of Earth & Atmospheric
Sciences
Saint Louis University
Saint Louis, MO 63156

Professor Bryan Isacks
Cornell University
Dept of Geological Sciences
SNEE Hall
Ithaca, NY 14850

Professor Lane R. Johnson
Seismographic Station
University of California
Berkeley, CA 94720

Professor Thomas H. Jordan
Department of Earth, Atmospheric
and Planetary Sciences
Mass Institute of Technology
Cambridge, MA 02139

Dr. Alan Kafka
Department of Geology &
Geophysics
Boston College
Chestnut Hill, MA 02167

Professor Leon Knopoff
University of California
Institute of Geophysics
& Planetary Physics
Los Angeles, CA 90024

Professor Charles A. Langston
Geosciences Department
403 Deike Building
The Pennsylvania State University
University Park, PA 16802

Professor Thorne Lay
Department of Geological Sciences
1006 C.C. Little Building
University of Michigan
Ann Arbor, MI 48109-1063

Dr. Randolph Martin III
New England Research, Inc.
76 Olcott Drive
White River Junction, VT 05001

Dr. Gary McCartor
Mission Research Corp.
735 State Street
P.O. Drawer 719
Santa Barbara, CA 93102 (2 copies)

Professor Thomas V. McEvilly
Seismographic Station
University of California
Berkeley, CA 94720

Dr. Keith L. McLaughlin
S-CUBED,
A Division of Maxwell Laboratory
P.O. Box 1620
La Jolla, CA 92038-1620

Professor William Menke
Lamont-Doherty Geological Observatory
of Columbia University
Palisades, NY 10964

Professor Brian J. Mitchell
Department of Earth & Atmospheric
Sciences
Saint Louis University
Saint Louis, MO 63156

Mr. Jack Murphy
S-CUBED, A Division of Maxwell Lab
11800 Sunrise Valley Drive
Suite 1212
Reston, VA 22091 (2 copies)

Professor J. A. Orcutt
IGPP, A-205
Scripps Institute of Oceanography
Univ. of California, San Diego
La Jolla, CA 92093 La Jolla, CA 92093

Professor Keith Priestley
University of Nevada
Mackay School of Mines
Reno, NV 89557

Professor Paul G. Richards
Lamont-Doherty Geological
Observatory of Columbia Univ.
Palisades, NY 10964

Wilmer Rivers
Teledyne Geotech
314 Montgomery Street
Alexandria, VA 22314

Dr. Alan S. Ryall, Jr.
Center of Seismic Studies
1300 North 17th Street
Suite 1450
Arlington, VA 22209-2308 (4 copies)

Professor Charles G. Sammis
Center for Earth Sciences
University of Southern California
University Park
Los Angeles, CA 90089-0741

Professor Christopher H. Scholz
Geological Sciences
Lamont-Doherty Geological Observatory
Palisades, NY 10964

Dr. Jeffrey L. Stevens
S-CUBED,
A Division of Maxwell Laboratory
P.O. Box 1620
La Jolla, CA 92038-1620

Professor Brian Stump
Institute for the Study of Earth & Man
Geophysical Laboratory
Southern Methodist University
Dallas, TX 75275

Professor Ta-liang Teng
Center for Earth Sciences
University of Southern California
University Park
Los Angeles, CA 90089-0741

Dr. Clifford Thurber
State University of New York at
Stony Brook
Dept of Earth and Space Sciences
Stony Brook, NY 11794-2100

Professor M. Nafi Toksoz
Earth Resources Lab
Massachusetts Institute of Technology
42 Carleton Street
Cambridge, MA 02142

Professor Terry C. Wallace
Department of Geosciences
Building #77
University of Arizona
Tucson, AZ 85721

Weidlinger Associates
ATTN: Dr. Gregory Wojcik
4410 El Camino Real, Suite 110
Los Altos, CA 94022

Professor Francis T. Wu
Department of Geological Sciences
State University of New York
at Binghamton
Vestal, NY 13901

Dr. Monem Abdel-Gawad
Rockwell Internat'l Science Center
1049 Camino Dos Rios
Thousand Oaks, CA 91360

Professor Shelton S. Alexander
Geosciences Department
403 Deike Building
The Pennsylvania State University
University Park, PA 16802

Dr. Ralph Archuleta
Department of Geological Sciences
Univ. of California at
Santa Barbara
Santa Barbara, CA

J. Barker
Department of Geological Sciences
State University of New York
at Binghamton
Vestal, NY 13901

Mr. William J. Best
907 Westwood Drive
Vienna, VA 22180

Dr. N. Biswas
Geophysical Institute
University of Alaska
Fairbanks, AK 99701

Dr. G. A. Bollinger
Department of Geological Sciences
Virginia Polytechnical Institute
21044 Derring Hall
Blacksburg, VA 24061

Mr. Roy Burger
1221 Serry Rd.
Schenectady, NY 12309

Dr. Robert Burridge
Schlumberger-Doll Resch Ctr.
Old Quarry Road
Ridgefield, CT 06877

Science Horizons, Inc.
ATTN: Dr. Theodore Cherry
710 Encinitas Blvd., Suite 200
Encinitas, CA 92024 (2 copies)

Professor Jon F. Claerbout
Professor Amos Nur
Dept. of Geophysics
Stanford University
Stanford, CA 94305 (2 copies)

Dr. Anton W. Dainty
Earth Resources Lab
Massachusetts Institute of Technology
42 Carleton Street
Cambridge, MA 02142

Professor Adam Dziewonski
Hoffman Laboratory
Harvard University
20 Oxford St.
Cambridge, MA 02138

Professor John Ebel
Dept of Geology and Geophysics
Boston College
Chestnut Hill, MA 02167

Dr. Donald Forsyth
Dept of Geological Sciences
Brown University
Providence, RI 02912

Dr. Anthony Gangi
Texas A&M University
Department of Geophysics
College Station, TX 77843

Dr. Freeman Gilbert
Inst. of Geophysics & Planetary Physics
University of California, San Diego
P.O. Box 109
La Jolla, CA 92037

Mr. Edward Giller
Pacific Seirra Research Corp.
1401 Wilson Boulevard
Arlington, VA 22209

Dr. Jeffrey W. Given
Sierra Geophysics
11255 Kirkland Way
Kirkland, WA 98033

Rong Song Jih
Teledyne Geotech
314 Montgomery Street
Alexandria, VA 22314

Professor F.K. Lamb
Univ. of Illinois at Urbana-Champaign
Department of Physics
1110 West Green Street
Urbana, IL 61801

Dr. Arthur Lerner-Lam
Lamont-Doherty Geological Observatory
of Columbia University
Palisades, NY 10964

Dr. L. Timothy Long
School of Geophysical Sciences
Georgia Institute of Technology
Atlanta, GA 30332

Dr. Peter Malin
University of California at
Santa Barbara
Institute for Central Studies
Santa Barbara, CA 93106

Dr. George R. Mellman
Sierra Geophysics
11255 Kirkland Way
Kirkland, WA 98033

Dr. Bernard Minster
IGPP, A-205
Scripps Institute of Oceanography
Univ. of California, San Diego
La Jolla, CA 92093

Professor John Nabelek
College of Oceanography
Oregon State University
Corvallis, OR 97331

Dr. Geza Nagy
U. California, San Diego
Dept of Ames, M.S. B-010
La Jolla, CA 92093

Dr. Jack Oliver
Department of Geology
Cornell University
Ithaca, NY 14850

Dr. Robert Phinney/Dr. F. A. Dahlen
Dept of Geological
Geological Science University
Princeton University
Princeton, NJ 08540

RADIX System, Inc.
Attn: Dr. Jay Pulli
2 Taft Court, Suite 203
Rockville, Maryland 20850

Dr. Norton Rimer
S-CUBED
A Division of Maxwell Laboratory
P.O. 1620
La Jolla, CA 92038-1620

Professor Larry J. Ruff
Department of Geological Sciences
1006 C.C. Little Building
University of Michigan
Ann Arbor, MI 48109-1063

Dr. Richard Sailor
TASC Inc.
55 Walkers Brook Drive
Reading, MA 01867

Thomas J. Sereno, Jr.
Science Application Int'l Corp.
10210 Campus Point Drive
San Diego, CA 92121

Dr. David G. Simpson
Lamont-Doherty Geological Observ.
of Columbia University
Palisades, NY 10964

Dr. Bob Smith
Department of Geophysics
University of Utah
1400 East 2nd South
Salt Lake City, UT 84112

Dr. S. W. Smith
Geophysics Program
University of Washington
Seattle, WA 98195

Dr. Stewart Smith
IRIS Inc.
1616 N. Fort Myer Drive
Suite 1440
Arlington, VA 22209

Rondout Associates
ATTN: Dr. George Sutton,
Dr. Jerry Carter, Dr. Paul Pomeroy
P.O. Box 224
Stone Ridge, NY 12484 (4 copies)

Dr. L. Sykes
Lamont Doherty Geological Observ.
Columbia University
Palisades, NY 10964

Dr. Pradeep Talwani
Department of Geological Sciences
University of South Carolina
Columbia, SC 29208

Dr. R. B. Tittmann
Rockwell International Science Center
1049 Camino Dos Rios
P.O. Box 1085
Thousand Oaks, CA 91360

Dr. Gregory van der Vink
IRIS, Inc.
1616 No. Fort Myer Drive
Suite 1440
Arlington, VA 22209

Professor John H. Woodhouse
Hoffman Laboratory
Harvard University
20 Oxford St.
Cambridge, MA 02138

Dr. Gregory B. Young
ENSCO, Inc.
5400 Port Royal Road
Springfield, VA 22151-2388

FOREIGN (OTHERS)

Dr. Peter Basham
Earth Physics Branch
Geological Survey of Canada
1 Observatory Crescent
Ottawa, Ontario, CANADA K1A OY3

Professor Ari Ben-Menahem
Dept of Applied Mathematics
Weizman Institute of Science
Rehovot
ISRAEL 951729

Dr. Eduard Berg
Institute of Geophysics
University of Hawaii
Honolulu, HI 96822

Dr. Michel Bouchon
I.R.I.G.M-B.P.
38402 St. Martin D'Heres
Cedex FRANCE

Dr. Hilmar Bungum/NTNF/NORSAR
P.O. Box 51
Norwegian Council of Science,
Industry and Research, NORSAR
N-2007 Kjeller, NORWAY

Dr. Michel Campillo
I.R.I.G.M.-B.P. 68
38402 St. Martin D'Heres
Cedex, FRANCE

Dr. Kin-Yip Chun
Geophysics Division
Physics Department
University of Toronto
Ontario, CANADA M5S 1A7

Dr. Alan Douglas
Ministry of Defense
Blacknest, Br[illegible]ton,
Reading RG7-[illegible]
UNITED KINGDOM

Dr. Manfred Henger
Fed. Inst. For Geosciences & Nat'l Res.
Postfach 510153
D-3000 Hannover 51
FEDERAL REPUBLIC OF GERMANY

Ms. Eva Johannisson
Senior Research Officer
National Defense Research Inst.
P.O. Box 27322
S-102 54 Stockholm, SWEDEN

Tormod Kvaerna
NTNF/NORSAR
P.O. Box 51
N-2007 Kjeller, NORWAY

Mr. Peter Marshall, Procurement
Executive, Ministry of Defense
Blacknest, Brimpton,
Reading FG7-4RS
UNITED KINGDOM (3 copies)

Dr. Robert North
Geophysics Division
Geological Survey of Canada
1 Observatory crescent
Ottawa, Ontario, CANADA K1A OY3

Dr. Frode Ringdal
NTNF/NORSAR
P.O. Box 51
N-2007 Kjeller, NORWAY

Dr. Jorg Schlittenhardt
Fed. Inst. for Geosciences & Nat'l Res.
Postfach 510153
D-3000 Hannover 51
FEDERAL REPUBLIC OF GERMANY

University of Hawaii
Institute of Geophysics
ATTN: Dr. Daniel Walker
Honolulu, HI 96822

Dr. Ramon Cabre, S.J.
Observatorio San Calixto
Casilla 5939
La Paz Bolivia

Professor Peter Harjes
Institute for Geophysik
Rhur University/Bochum
P.O. Box 102148, 4630 Bochum 1
FEDERAL REPUBLIC OF GERMANY

Dr. E. Husebye
NTNF/NORSAR
P.O. Box 51
N-2007 Kjeller, NORWAY

Professor Brian L.N. Kennett
Research School of Earth Sciences
Institute of Advanced Studies
G.P.O. Box 4
Canberra 2601, AUSTRALIA

Dr. B. Massinon
Societe Radiomana
27, Rue Claude Bernard
75005, Paris, FRANCE (2 copies)

Dr. Pierre Mechler
Societe Radiomana
27, Rue Claude Bernard
75005, Paris, FRANCE

Dr. Svein Mykkeltveit
NTNF/NORSAR
P.O. Box 51
N-2007 Kjeller, NORWAY (3 copies)

Dr. Ralph Alewine III
DARPA/NMRO
1400 Wilson Boulevard
Arlington, VA 22209-2308

Dr. Robert Blandford
DARPA/NMRO
1400 Wilson Boulevard
Arlington, VA 22209-2308

Sandia National Laboratory
ATTN: Dr. H. B. Durham
Albuquerque, NM 87185

Dr. Jack Evernden
USGS-Earthquake Studies
345 Middlefield Road
Menlo Park, CA 94025

U.S. Geological Survey
ATTN: Dr. T. Hanks
Nat'l Earthquake Resch Center
345 Middlefield Road
Menlo Park, CA 94025

Dr. James Hannon
Lawrence Livermore Nat'l Lab.
P.O. Box 808
Livermore, CA 94550

Paul Johnson
ESS-4, Mail Stop J979
Los Alamos National Laboratory
Los Alamos, NM 87545

Ms. Ann Kerr
DARPA/NMRO
1400 Wilson Boulevard
Arlington, VA 22209-2308

Dr. Max Koontz
US Dept of Energy/DP 5
Forrestal Building
1000 Independence Ave.
Washington, D.C. 20585

Dr. W. H. K. Lee
Office of Earthquakes, Volcanoes,
& Engineering
345 Middlefield Rd
Menlo Park, CA 94025

Dr. William Leith
U.S. Geological Survey
Mail Stop 928
Reston, VA 22092

Dr. Richard Lewis
Dir. Earthquake Engrg & Geophysics
U.S. Army Corps of Engineers
Box 631
Vicksburg, MS 39180

Dr. Robert Masse'
Box 25046, Mail Stop 967
Denver Federal Center
Denver, CO 80225

Richard Morrow
ACDA/VI
Room 5741
320 21st Street N.W.
Washington, D.C. 20451

Dr. Keith K. Nakanishi
Lawrence Livermore National Laboratory
P.O. Box 808, L-205
Livermore, CA 94550 (2 copies)

Dr. Carl Newton
Los Alamos National Lab.
P.O. Box 1663
Mail Stop C335, Group ESS-3
Los Alamos, NM 87545

Dr. Kenneth H. Olsen
Los Alamos Scientific Lab.
P.O. Box 1663
Mail Stop C335, Group ESS-3
Los Alamos, NM 87545

Howard J. Patton
Lawrence Livermore National Laboratory
P.O. Box 808, L-205
Livermore, CA 94550

Mr. Chris Paine
Office of Senator Kennedy
SR 315
United States Senate
Washington, D.C. 20510

AFOSR/NP
ATTN: Colonel Jerry J. Perrizo
Bldg 410
Bolling AFB, Wash D.C. 20332-6448

HQ AFTAC/TT
Attn: Dr. Frank F. Pilotte
Patrick AFB, Florida 32925-6001

Mr. Jack Rachlin
USGS - Geology, Rm 3 C136
Mail Stop 928 National Center
Reston, VA 22092

Robert Reinke
AFWL/NTESG
Kirtland AFB, NM 87117-6008

Dr. Byron Ristvet
HQ DNA, Nevada Operations Office
Attn: NVCG
P.O. Box 98539
Las Vegas, NV 89193

HQ AFTAC/TGR
Attn: Dr. George H. Rothe
Patrick AFB, Florida 32925-6001

Donald L. Springer
Lawrence Livermore National Laboratory
P.O. Box 808, L-205
Livermore, CA 94550

Dr. Lawrence Turnbull
OSWR/NED
Central Intelligence Agency
CIA, Room 5G48
Washington, D.C. 20505

Dr. Thomas Weaver
Los Alamos National Laboratory
P.O. Box 1663
MS C 335
Los Alamos, NM 87545

GL/SULL
Research Library
Hanscom AFB, MA 01731-5000 (2 copies)

Secretary of the Air Force (SAFRD)
Washington, DC 20330
Office of the Secretary Defense
DDR & E
Washington, DC 20330

HQ DNA
ATTN: Technical Library
Washington, DC 20305

DARPA/RMO/RETRIEVAL
1400 Wilson Blvd.
Arlington, VA 22209

DARPA/RMO/Security Office
1400 Wilson Blvd.
Arlington, VA 22209

GL/XO
Hanscom AFB, MA 01731-5000

GL/LW
Hanscom AFB, MA 01731-5000

DARPA/PM
1400 Wilson Boulevard
Arlington, VA 22209

Defense Technical
Information Center
Cameron Station
Alexandria, VA 22314
(5 copies)

Defense Intelligence Agency
Directorate for Scientific &
Technical Intelligence
Washington, D.C. 20301

Defense Nuclear Agency/SPSS
ATTN: Dr. Michael Shore
6801 Telegraph Road
Alexandria, VA 22310

AFTAC/CA (STINFO)
Patrick AFB, FL 32925-6001

Mr. Alfred Lieberman
ACDA/VI-OA'State Department Building
Room 5726
320 - 21St Street, NW
Washington, D.C. 20451

TACTEC
Battelle Memorial Institute
505 King Avenue
Columbus, OH 43201 (Final report only)